



A general cocatalyst strategy for performance enhancement in nickel catalyzed ethylene (co)polymerization

Quan Wang, Zhao Zhang, Chen Zou*, Changle Chen*

CAS Key Laboratory of Soft Matter Chemistry, Department of Polymer Science and Engineering, University of Science and Technology of China, Hefei 230026, China

ARTICLE INFO

Article history:

Received 10 November 2021

Revised 6 December 2021

Accepted 15 December 2021

Available online 20 December 2021

Keywords:

Nickel

Cocatalyst

Magnesium

Ethylene polymerization

ABSTRACT

The tuning of olefin-polymerization catalyst properties through ligand modifications is efficient but requires complicated and costly syntheses. In this contribution, a simple Bu_2Mg -based cocatalyst strategy is designed that can simultaneously enhance the catalytic properties (activity, thermal stability, polymer molecular weight, branching density, melting point, *etc.*) of various nickel catalysts (α -diimine nickel, pyridine imine nickel and iminopyridine-*N*-oxide nickel) in ethylene polymerization, and enable great product morphology control. For example, a simple α -diimine nickel catalyst can demonstrate polymerization activity of up to $1.29 \times 10^7 \text{ g mol}^{-1} \text{ h}^{-1}$ and molecular weight of up to $1.90 \times 10^6 \text{ g/mol}$ in the presence of Bu_2Mg cocatalyst. The resulting polyethylenes exhibit excellent mechanical properties, with tensile stress of up to 47.4 MPa and strain of up to 1020%. This cocatalyst strategy is generally applicable to different nickel catalysts, and can lead to property enhancement in ethylene copolymerization with a series of polar comonomers such as methyl 10-undecylenate, 10-undecylenic acid and 10-undecenol.

© 2022 Published by Elsevier B.V. on behalf of Chinese Chemical Society and Institute of Materia Medica, Chinese Academy of Medical Sciences.

In 1963, Ziegler and Natta won the Nobel Prize for their contributions to olefin polymerization catalysts. More than 50 years later, polyolefins are widely used in both industry and everyday products due to their desirable properties and low cost. The design and development of high-performance catalysts have attracted great attention from both academia and industry [1–16]. Since Brookhart's seminal works on α -diimine catalyst (Scheme 1, **A**) [17], this catalyst system has been extensively investigated in the past few decades [18–25]. Due to their unique chain walking mechanism, this type of catalysts can prepare polyolefins with branched chain structures and various polymer topologies. However, many of the initially reported α -diimine catalysts suffered from low thermal stability, which prevents their potential industrial applications.

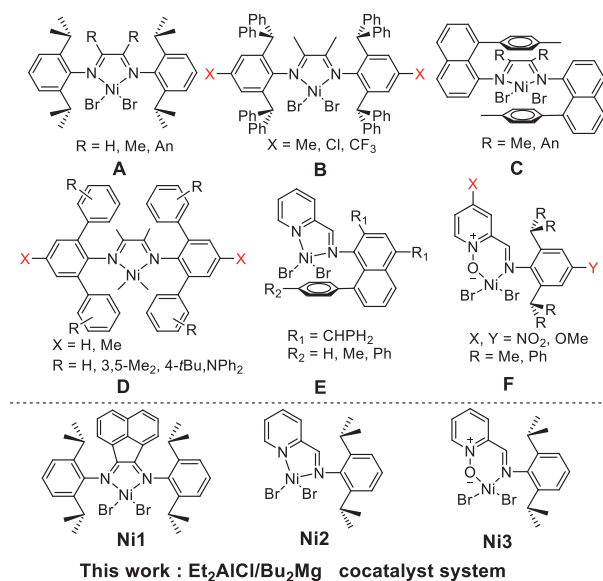
Generally, modifications on ligand steric hindrance and electronic effects can improve important parameters such as activity, thermal stability and polymer molecular weight. For instance, Long and coworkers reported the studies of an α -diimine Ni(II) catalyst (Scheme 1, **B**) containing benzhydryl moiety, which maintained high activity at temperatures up to 100 °C [26]. Chen and coworkers studied ligand electronic effect on ethylene polymerization catalyzed by α -diimine nickel(II), which can efficiently influence cat-

alytic activity and polyethylene molecular weight [27]. Brookhart, Daugulis and Coates designed a “sandwich-type” α -diimine nickel catalyst (Scheme 1, **C**) with great properties in ethylene polymerization. These catalysts possess increased axial bulkiness, resulting in lower rates of chain transfer relative to chain propagation rates [28–30].

Rieger and coworkers prepared a series of Ni(II) catalysts with meta-substituted terphenyl α -diimine ligands (Scheme 1, **D**), which afforded highly linear polyethylenes [31]. Recently, Jian and coworkers designed a concerted double-layer steric strategy by interlocking the axial spaces around the metal center to form a large blockage, enabling high activity (up to $1.03 \times 10^9 \text{ g mol}^{-1} \text{ h}^{-1}$) and high polymer molecular weight ($M_w = 4.2 \times 10^6 \text{ g/mol}$) [32]. In addition to the developments in α -diimine nickel system, a series of nickel catalysts bearing new ligands have been designed and synthesized. For example, Chen and coworkers prepared a series of iminopyridyl Ni(II) catalysts (Scheme 1, **E**) containing both dibenzhydryl and naphthyl moieties, generating polyethylene with molecular weight of up to one million [33]. Similarly, some iminopyridine-*N*-oxide nickel catalysts have been demonstrated with great properties in ethylene polymerization (Scheme 1, **F**). It was shown that the steric hindrance and electronic effect of the ligand can significantly improve the polymerization activity, and ultra-high molecular weight polyethylene with tunable molecular weight distribution can be obtained [34–36].

* Corresponding authors.

E-mail addresses: chen1215@mail.ustc.edu.cn (C. Zou), changle@ustc.edu.cn (C. Chen).



Scheme 1. Selected examples of previously reported nickel catalysts, and the three nickel catalysts used in this work.

Modifications on ligand sterics and electronics have been widely used in tuning catalysts properties. However, this usually requires costly and cumbersome ligand/catalyst syntheses. Alternatively, the tuning of catalyst properties through different cocatalyst represents an easy and generally applicable strategy, which has been widely used in early transition metal-based olefin polymerization catalysts [37,38]. For example, the utilization of boranes [39–42], aluminum alkyls [43,44] or magnesium salts [45–47] cannot only influence the catalytic performances, but also act as support to modulate product morphology [48,49]. Product morphology control is a critical issue in polyolefin industry.

However, this cocatalyst strategy has remained largely unexplored in late transition metal-based olefin polymerization catalysts, especially for the purpose of product morphology control [50–56]. In this contribution, we decide to explore the influence of a Et₂AlCl/Bu₂Mg binary cocatalyst system on a known α -diimine Ni(II) catalyst (Scheme 1, **Ni1**). In addition to significantly improved catalytic activity and polymer molecular weight, this cocatalyst enables great product morphology control. More importantly, this strategy is generally applicable for various late transition metal nickel catalysts such as pyridine imine nickel (Scheme 1, **Ni2**) [57] and iminopyridine-*N*-oxide nickel (Scheme 1, **Ni3**) [58] catalysts.

Similar with literature reports, the activation of classic **Ni1** with Et₂AlCl catalyzes the polymerization of ethylene (30 °C, 50 °C and 80 °C) to generate branched polyethylene (the branching densities: 53–79/1000 C) with activities of ca. 10⁶ g mol⁻¹ h⁻¹ (Table 1, entries 1–3). In contrast, the addition of Bu₂Mg to Et₂AlCl followed by injection of the nickel catalyst can increase the polymerization activity to up to 1.29 × 10⁷ g mol⁻¹ h⁻¹ (Table 1, entries 4–10). The polyethylene molecular weight was increased by an order of magnitude from 1.72 × 10⁵ g/mol to 1.90 × 10⁶ g/mol. The polyethylene branching density was decreased from 53 to 10 per 1000 carbon atoms, along with significantly increased polymer melting point (from 85 °C to 129.7 °C). When the amount of Bu₂Mg was increased to be the same as or exceeding the amount of Et₂AlCl, the polymerization activity was significantly reduced (Table 1, entries 11 and 12). In another set of control experiment, the addition of Bu₂Mg to the nickel catalyst followed by injection of Et₂AlCl showed no activity at all (Table 1, entry 13). These results indicated that excessive Bu₂Mg may react with the nickel pre-catalyst and

deactivate the system. This performance enhancement was amplified at higher polymerization temperatures (Table 1, entries 14 and 15, Fig. S1a in Supporting information). For example, the polymerization activity and molecular weight were increased by 9 and 29 times, respectively, with the addition of 250 equiv. Bu₂Mg at 80 °C (Table 1, entry 15 vs. entry 3). Moreover, polymerization time dependence studies at 80 °C showed that the addition of Bu₂Mg can significantly increase catalyst thermal stability (Fig. S1b in Supporting information).

This Bu₂Mg-based cocatalyst strategy is also applicable in **Ni2** and **Ni3** systems. With the addition of Bu₂Mg, the polymerization activity of **Ni2** was increased by more than 10 times, along with increased polyethylene molecular weight, decreased branching density and increased melting point (Table 1, entries 16–18, Fig. S1c in Supporting information). The polymer molecular weight distribution was increased after adding Bu₂Mg, which may be caused by the generation of multiple active centers through interaction of the sterically open ligands with Bu₂Mg. With Et₂AlCl cocatalyst, **Ni3** is not active at all in ethylene polymerization (Table 1, entry 19). However, the addition of Bu₂Mg can lead to highly active catalyst (Table 1, entries 20 and 21).

The origin of this interesting Bu₂Mg-based cocatalyst strategy was investigated. The addition of Bu₂Mg to Et₂AlCl could lead to the formation of MgCl₂ [47], which serves as an efficiently solid support for nickel catalysts and influences their properties in polymerization. Scanning electron microscope showed the reaction of AlEt₂Cl with Bu₂Mg led to the formation of discrete particles with diameters of ca. 100 nm (Fig. 1a). The shape of the resulting polyethylene particles replicated that of MgCl₂ with average diameters increased to ca. 500 nm at 30 °C (Fig. 1b). Importantly, the polymers prepared in the presence of Bu₂Mg are in the form of dispersed and non-sticky particles (Fig. 1c). In direct contrast, the absence of Bu₂Mg results in the formation of viscous and continuous materials (Fig. 1d). Previously, it has been demonstrated that the supporting of homogeneous nickel catalysts on solid support usually led to increased polymer molecular weight and decreased branching density in ethylene polymerization [50–56]. This is consistent with our experimental results, and support the above-mentioned hypothesis. Most importantly, this simple cocatalyst strategy can prevent reactor fouling through polymer morphology control.

The influence of the Bu₂Mg on **Ni1** catalyzed ethylene-polar comonomer copolymerization was also investigated (Table 2). Under the current conditions, **Ni1** was not able to mediate ethylene copolymerization with methyl 10-undecenoate (Table 2, entry 1). In contrast, the addition of Bu₂Mg can enable efficient copolymerization (Table 2, entry 2), affording copolymers with high molecular weight (22.5 × 10⁴) and moderate comonomer incorporation (3.2%). For comonomers of 10-undecylenic acid and 10-undecenol, Bu₂Mg can significantly increase copolymer molecular weights, while slightly affect activity and comonomer incorporation (Table 2, entries 4–8). The resulting copolymers are amorphous in the absence of Bu₂Mg, while semicrystalline copolymers with high melting points can be generated with the addition of Bu₂Mg.

The influence of Bu₂Mg on polymer microstructures (molecular weight, branching density, etc.) can translate into influences on physical properties. Tensile tests were carried out to probe the mechanical properties of these polyethylene products (Fig. 1e). In the absence of Bu₂Mg, **Ni1** generated polyethylene with elastic properties (strength of 8.5 MPa and strain of 1400%). However, the addition of Bu₂Mg led to the formation of polyethylenes bearing hard and strong thermoplastic properties, with significantly enhanced tensile strength (33.2–47.4 MPa) and good strain values (830%–1030%). Polyethylene with good mechanical properties can be obtained even at 80 °C (sample from Table 1, entry 15). However, only sticky oil product can be obtained in the ab-

Table 1
Effect of the Bu₂Mg for nickel catalyst on ethylene polymerization.^a

Entry	Cat.	T (°C)	Bu ₂ Mg (equiv.)	Yield (g)	Act. ^b	T _m ^c (°C)	B ^d	M _n ^e	M _w /M _n ^e
1	Ni1	30	0	0.32	2.56	85.0	53	17.2	2.5
2	Ni1	50	0	0.19	1.52	–	54	14.6	2.4
3	Ni1	80	0	0.12	0.96	–	79	4.6	3.8
4	Ni1	30	50	1.01	8.08	118.3	28	88.7	4.0
5	Ni1	30	75	1.42	11.36	119.8	25	95.9	3.5
6	Ni1	30	125	1.39	11.12	122.1	24	106.4	3.2
7	Ni1	30	200	1.45	11.60	124.6	21	121.7	3.0
8	Ni1	30	250	1.62	12.96	127.1	15	142.7	2.1
9	Ni1	30	300	1.41	11.28	128.8	13	154.2	2.1
10	Ni1	30	400	0.71	5.68	129.7	10	190.1	2.1
11	Ni1	30	500	0.05	0.40	118.7	23	95.6	4.8
12	Ni1	30	600	trace	–	–	–	–	–
13 ^f	Ni1	30	250	trace	–	–	–	–	–
14	Ni1	50	250	1.02	8.16	126.6	16	97.8	1.9
15	Ni1	80	250	0.89	7.12	125.5	21	77.3	1.9
16	Ni2	30	0	0.05	0.40	64.3	56	0.3	1.7
17	Ni2	30	125	0.57	4.56	116.5	28	0.7	8.3
18	Ni2	30	250	0.64	5.12	119.7	42	0.5	5.3
19	Ni3	30	0	trace	–	–	–	–	–
20	Ni3	30	125	0.10	0.80	125.1	19	1.0	10.7
21	Ni3	30	250	0.04	0.32	124.7	15	1.1	9.0

^a Conditions: Catalyst 0.5 μmol, Et₂AlCl 500 equiv., P: 8 atm, t = 15 min, n-heptane 5 mL. A mixture of Et₂AlCl and Bu₂Mg was added to the polymerization reactor, followed by the injection of the nickel catalyst.

^b The overall activity (10⁶ g mol⁻¹ h⁻¹) was determined from the mass of the polymer product. Values are the average of at least two runs.

^c Determined by DSC.

^d Branches per 1000 carbon atoms, determined by ¹H NMR analysis.

^e M_n: 10⁴ g/mol, M_n and M_w/M_n determined by GPC in trichlorobenzene at 150 °C.

^f A mixture of Bu₂Mg and nickel catalyst was added to the polymerization reactor, followed by the injection of Et₂AlCl.

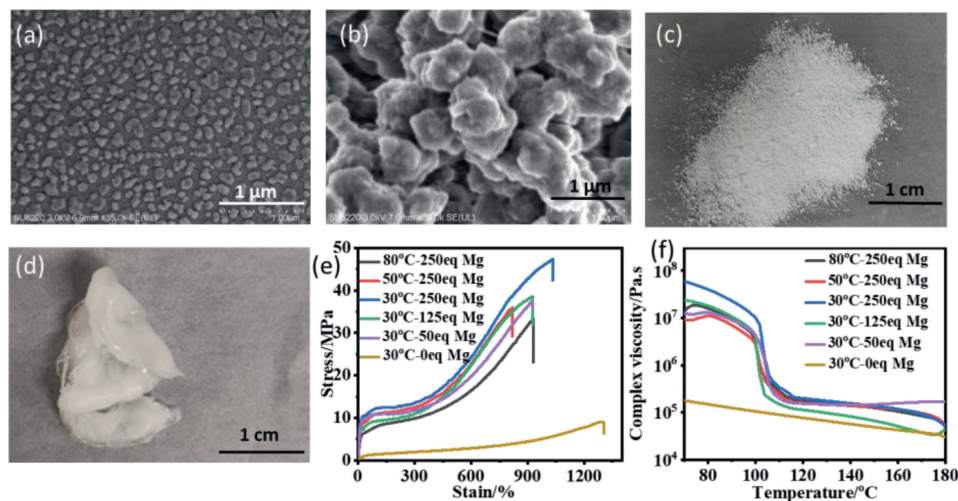


Fig. 1. (a) Scanning electron micrograph of the MgCl₂ particle formed from the reaction of Et₂AlCl with Bu₂Mg. (b) Scanning electron micrograph of the polymer products for entry 6. (c) The photograph of the polymer products from entry 8 (500 equiv. Et₂AlCl, 250 equiv. Bu₂Mg). (d) The photograph of the polymer products from entry 1 (500 equiv. Et₂AlCl, 0 equiv. Bu₂Mg). (e) Stress-strain curves of the polymer products from Ni1. (f) Complex viscosity curves of the polymer products from Ni1.

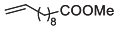
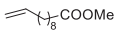
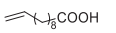
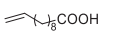
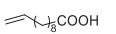
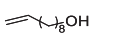
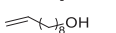
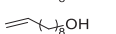
sence of Bu₂Mg. The outstanding mechanical properties of these polyethylenes can be attributed to their low branching density and high molecular weight.

Furthermore, the rheological behaviors of these polyethylenes were studied using flat plate rheometer. The storage modulus (*G'*) and complex viscosity are two important parameters related to polymer rheological and processing properties [59]. The complex viscosity was determined using temperature sweep experiments with Anton Paar MCR302 (plate: 25 mm diameter). The temperature scanning rate was set at 5 °C/min, and the frequency was set constant at 1.0 Hz (Fig. 1f). When the temperature was increased from 70 °C to 180 °C, the complex viscosities of samples prepared without Bu₂Mg (30 °C, 0 equiv. Bu₂Mg, Table 1, entry 1) decreased smoothly, indicating elastic properties. In contrast, a significant step change at approximately 100 °C were observed for the sam-

ples prepared in the presence of Bu₂Mg, which were characteristic of thermoplastics. These results are consistent with the previously mentioned polymer thermal properties and mechanical properties.

In summary, we have developed a simple and effective cocatalyst strategy to enhance the properties of nickel catalysts in ethylene polymerization. In addition to significantly improved activity, thermal stability, polymer molecular weight, greatly reduced branching density and increased melting points, this strategy enables great product morphology control. Moreover, the polyethylene products prepared by this strategy possess good mechanical properties and tunable rheological/processing properties. Similar property enhancement was also observed in ethylene copolymerization with a series of polar comonomers such as methyl 10-undecylenate, 10-undecylenic acid and 10-undecenol. Most importantly, this versatile strategy is generally applicable to different

Table 2
Influence of the Bu₂Mg on NiI catalyzed ethylene-polar comonomer copolymerization.^a

Entry	Comonomer	[M] (mol/L)	Bu ₂ Mg (equiv.)	Yield (g)	Act. ^b	T _m ^c (°C)	Incorp. mol. (%) ^d	M _n ^e	M _w /M _n ^e
1		0.2	0	trace	–	–	–	–	–
2		0.2	250	0.26	0.42	122.5	3.2	22.5	4.5
3		0.2	0	2.50	5.00	–	2.8	11.5	4.4
4		0.2	250	2.41	4.82	121.1	0.6	37.4	4.5
5		0.5	250	1.45	2.90	118.0	1.4	20.9	4.5
6		0.2	0	2.58	5.16	–	1.1	24.6	4.5
7		0.2	250	2.71	5.42	119.8	0.5	84.4	4.6
8		0.5	250	1.53	3.06	116.7	1.2	40.0	6.4

^a Conditions: Catalyst NiI 10 μmol, 30 °C, 8 atm, Et₂AlCl: 1000 equiv., Bu₂Mg: 250 equiv., 20 mL *n*-heptane, *t* = 30 min.^b Activity: 10⁵ g mol⁻¹ h⁻¹. Values are the average of at least two runs.^c Determined by DSC.^d Determined by ¹H NMR analysis.^e M_n: 10⁴ g/mol, M_n and M_w/M_n determined by GPC in trichlorobenzene at 150 °C.

nickel catalyst systems. It is expected that further studies using different cocatalysts and on different late transition metal catalysts could lead to the discovery of superior systems with potentials for practical applications.

Declaration of competing interest

The authors declare that they have no known competing financial interests or personal relationships that could have appeared to influence the work reported in this paper.

Acknowledgments

This work was supported by National Key R&D Program of China (No. 2021YFA1501700), National Natural Science Foundation of China (Nos. 52025031, U19B6001 and U1904212) and K. C. Wong Education Foundation.

Supplementary materials

Supplementary material associated with this article can be found, in the online version, at doi:10.1016/j.ccl.2021.12.036.

References

- [1] C.L. Chen, Nat. Rev. Chem. 2 (2018) 6–14.
- [2] Y.S. Gao, J.Z. Chen, Y. Wang, et al., Nat. Catal. 2 (2019) 236–242.
- [3] J.M. Eagan, J. Xu, R.D. Girolamo, et al., Science 355 (2017) 814–816.
- [4] H.L. Mu, G.L. Zhou, X.Q. Hu, Z.B. Jian, Coord. Chem. Rev. 435 (2021) 213802.
- [5] S. Behzadi, C. Zou, B.P. Yang, C. Tan, C.L. Chen, Chin. J. Polym. Sci. 39 (2021) 447–454.
- [6] M.H. Xu, C.L. Chen, Sci. Bull. 66 (2021) 1429–1436.
- [7] L. Zhong, H.D. Zheng, C. Du, et al., J. Catal. 384 (2020) 208–217.
- [8] X. Fu, L.J. Zhang, R. Tanaka, T. Shiono, Z.G. Cai, Macromolecules 50 (2017) 9216–9221.
- [9] H. Zhang, C. Zou, H. Zhao, Z.G. Cai, C.L. Chen, Angew. Chem. Int. Ed. 60 (2021) 17446–17451.
- [10] X.L. Wang, Y.P. Zhang, F. Wang, et al., ACS Catal. 11 (2021) 2902–2911.
- [11] S.L.J. Luckham, K. Nozaki, Acc. Chem. Res. 54 (2021) 344–355.
- [12] C. Tan, C.L. Chen, Angew. Chem. Int. Ed. 58 (2019) 7192–7200.
- [13] Z. Chen, M. Brookhart, Acc. Chem. Res. 51 (2018) 1831–1839.
- [14] S. Mecking, M. Schmitte, Acc. Chem. Res. 53 (2020) 2738–2752.
- [15] S.Y. Chen, R.C. Pan, M. Chen, et al., J. Am. Chem. Soc. 143 (2021) 10743–10750.
- [16] M. Stürzel, S. Mihan, R. Mülhaupt, Chem. Rev. 116 (2016) 1398–1433.
- [17] L.K. Johnson, C.M. Killian, M. Brookhart, J. Am. Chem. Soc. 117 (1995) 6414–6415.
- [18] L.K. Johnson, S. Mecking, M. Brookhart, J. Am. Chem. Soc. 118 (1996) 267–268.
- [19] D. Takeuchi, Polym. J. 50 (2018) 573–578.
- [20] F.Z. Wang, C.L. Chen, Polym. Chem. 10 (2019) 2354–2369.
- [21] J.M. Kaiser, B.K. Long, Coord. Chem. Rev. 372 (2018) 141–152.
- [22] D. Peng, C.L. Chen, Angew. Chem. Int. Ed. 60 (2021) 22195–22200.
- [23] G.H. Wang, D. Peng, Y. Sun, C.L. Chen, CCS Chem. 2 (2020) 2025–2034.
- [24] Q. Muhammad, C. Tan, C.L. Chen, Sci. Bull. 65 (2020) 300–307.
- [25] C. Tan, C.L. Chen, Sci. Bull. 65 (2020) 1137–1138.
- [26] J.L. Rhinehart, L.A. Brown, B.K. Long, J. Am. Chem. Soc. 135 (2013) 16316–16319.
- [27] L.H. Guo, S.Y. Dai, C.L. Chen, Polymers 8 (2016) 37.
- [28] D. Zhang, E.T. Nadres, M. Brookhart, O. Daugulis, Organometallics 32 (2013) 5136–5143.
- [29] O. Padilla-Vélez, K.S. O'Connor, A.M. Lapointe, S.N. Macmillan, G.W. Coates, Chem. Commun. 55 (2019) 7607–7610.
- [30] K.S. O'Connor, A. Watts, T. Vaidya, et al., Macromolecules 49 (2016) 6743–6751.
- [31] M. Schmid, R. Eberhardt, M. Klinga, M. Leskelä, B. Rieger, Organometallics 20 (2001) 2321–2330.
- [32] J. Xia, Y.X. Zhang, S.Q. Kou, Z.B. Jian, J. Catal. 390 (2020) 30–36.
- [33] S.Y. Dai, X.L. Sui, C.L. Chen, Chem. Commun. 52 (2016) 9113–9116.
- [34] M.J. Chi, A. Chen, W.M. Pang, C. Tan, C.L. Chen, Chin. J. Chem. 39 (2021) 1683–1689.
- [35] C. Zou, S.Y. Dai, C.L. Chen, Macromolecules 51 (2018) 49–56.
- [36] M. Brasse, J. Cámpora, P. Palma, et al., Organometallics 27 (2008) 4711–4723.
- [37] E.Y. Chen, T.J. Marks, Chem. Rev. 100 (2000) 1391–1434.
- [38] L. Li, M.V. Metz, H. Li, et al., J. Am. Chem. Soc. 124 (2002) 12725–12741.
- [39] T. Nakashima, Y. Nakayama, T. Shiono, R. Tanaka, ACS Catal. 11 (2021) 865–870.
- [40] J.Z. Chen, A. Motta, B.H. Wang, Y.S. Gao, T.J. Marks, Angew. Chem. Int. Ed. 58 (2019) 7030–7034.
- [41] H. Li, L. Li, T.J. Marks, L. Liable-Sands, A.L. Rheingold, J. Am. Chem. Soc. 125 (2003) 10788–10789.
- [42] C.L. Beswick, T.J. Marks, J. Am. Chem. Soc. 122 (2000) 10358–10370.
- [43] W.P. Zheng, A.H. He, C.G. Liu, H.F. Shao, R.G. Wang, Polymer 210 (2020) 122998.
- [44] M.A. Akram, X. Liu, B. Jiang, et al., J. Macromol. Sci. A. 58 (2021) 539–549.
- [45] R. Huang, F. Malizia, G. Pennini, C.E. Koning, J.C. Chadwick, Macromol. Rapid. Comm. 29 (2008) 1732–1738.
- [46] V.A. Tuskaev, S.C. Gagieva, D.A. Kurmaev, et al., Chin. J. Polym. Sci. 37 (2019) 471–477.
- [47] Y.V. Kissin, R.I. Mink, A.J. Brandolini, T.E. Nowlin, J. Polym. Sci. 47 (2009) 3271–3285.
- [48] D. Liu, S.A. Lin, F.M. Zhu, H.Y. Gao, Q. Wu, Polym. Bull. 61 (2008) 71–80.
- [49] Y. Nakayama, H. Bando, Y. Sonobe, et al., J. Catal. 215 (2003) 171–175.
- [50] J.R. Severn, J.C. Chadwick, V.V.A. Castelli, Macromolecules 37 (2004) 6258–6259.
- [51] F. Yu, P. Li, M.L. Xu, et al., Polymer 229 (2021) 124023.
- [52] R.W. Xu, D.B. Liu, S.B. Wang, B.Q. Mao, Macromol. Chem. Phys. 207 (2006) 779–786.
- [53] P. Preishuber-Pflugl, M. Brookhart, Macromolecules 35 (2002) 6074–6076.
- [54] H.S. Schrekker, V. Kotov, P. Preishuber-Pflugl, P. White, M. Brookhart, Macromolecules 39 (2006) 6341–6354.
- [55] M. Okada, Y. Nakayama, T. Shiono, Macromol. Chem. Phys. 215 (2014) 1792–1796.
- [56] T. Liang, S. Goudari, C.L. Chen, Nat. Commun. 11 (2020) 372–380.
- [57] Z. Chen, K.E. Allen, P.S. White, O. Daugulis, M. Brookhart, Organometallics 35 (2016) 1756–1760.
- [58] M. Brasse, J. Cámpora, P. Palma, E. A'lvarez, Organometallics 27 (2008) 4711–4723.
- [59] D.J. Lohse, S.T. Milner, L.J. Fetters, et al., Macromolecules 35 (2002) 3066–3075.